Second International Symposium on Marine Propulsors
smp'11, Hamburg, Germany, June 2011
Workshop: Propeller performance

Performance and Cavitation Evaluation of Marine Propeller using Numerical Simulations

Keita Fujiyama[1], Chuel-Ho Kim[1], Daisuke Hitomi[1]

[1]Software Cradle Co., Ltd., Osaka, JAPAN

ABSTRACT

SC/Tetra is general purpose computational fluid dynamics (CFD) software using unstructured mesh finite volume method. SC/Tetra implements both the RANS-based turbulence model for the transitional flows and the model for cavitating-flows. In this paper, the problems provided by SMP'11 workshop are solved, and the accuracy and reliability of SC/Tetra were evaluated by analyzing the flows on marine propellers based on the results of the problems.

First, numerical simulations of non-cavitating flow, i.e., open water tests, were performed by using the LKE k-k_L-ω model and the transitional flow behaviors on the propeller surface were analyzed.

Next, numerical simulations of cavitating flow were conducted by using the full-cavitation model and the cavity patterns, especially the tip vortex, obtained from the simulations were compared.

Then, all results obtained from the simulations shows that the RANS-based CFD code, SC/Tetra, is effective for the numerical simulations of both non-cavitating and cavitating flows on marine propellers. .

Keywords

Numerical Simulation, Transitional Flow, Cavitation

1 INTRODUCTION

SC/Tetra, developed by Software Cradle Co., Ltd. in Japan from 2001, is general purpose CFD software using unstructured mesh finite volume method. SC/Tetra intends to be a design tool for mechanical engineers and designers, and is widely used mainly by the users in the automotive, electrical appliance, turbo-machinery fields.

With the development of computer technology, CFD is being introduced in the marine propulsion field. They require large-scale simulations such as cavitation analyses and SC/Tetra offers the solution. More and more companies in the marine propulsion filed can be SC/Tetra users.

The latest SC/Tetra Version 9 will be released in July 2011, and the following new features are incorporated:

- RANS based LKE k-k_L-ω turbulence model for simulations of transitional flows
- Full cavitation model

These new features enable the user to analyse marine propellers more efficiently and effectively compared with the conventional functions of SC/Tetra.

The problems of SMP'11 workshops were solved by using the aforementioned two new methods as well as other methods incorporated in SC/Tetra. The accuracy and reliability of SC/Tetra were evaluated based on the obtained results.

2 NUMERICAL MODEL

Our commercial CFD software SC/Tetra version 9 was used for all simulations presented in this paper. SC/Tetra, which is the finite volume solver for general purpose, implements low-Reynolds-number type turbulence models, cavitation models, a moving mesh method etc.

In this paper, we used the LKE k-k_L-ω model, which can simulate transitional flows, for analyses of open water tests. Additionally, we used the full-cavitation model for the simulations of cavitating flows.

2.1 Predictions of Transitional Flows

It is important to know the transition point of a flow around an object, especially low-Reynolds-number flow such as the flow around MAV (micro air vehicle) and the flows of the open water tests. LKE (Laminar Kinetic Energy) model (Walters & Leylek 2004) is one of RANS (Reynolds-averaged Navier-Stokes) based approaches to simulate the transitional flow.

In the LKE model, the disturbance energy in a pre-transitional region of a boundary layer is represented as Laminar Kinetic Energy (k_L), while the turbulence energy

is as k. The transport equation of k_L is solved by using two equations of fully turbulent model. SC/Tetra introduces the following k-k_L-ω model (Walters & Cokljat 2008) which was developed based on the k-ω model:

$$\frac{\partial \rho k}{\partial t}+\frac{\partial u_i \rho k}{\partial x_i}=\rho(P_k+R_{BP}+R_{NAT}-\omega k-D_T)+\frac{\partial}{\partial x_i}\left[\left(\mu+\frac{\rho\alpha_T}{\sigma_k}\right)\frac{\partial k}{\partial x_i}\right] \quad (1)$$

$$\frac{\partial \rho k_L}{\partial t}+\frac{\partial u_i \rho k_L}{\partial x_i}=\rho(P_{kL}-R_{BP}-R_{NAT}-D_L)+\frac{\partial}{\partial x_i}\left[\mu\frac{\partial k_L}{\partial x_i}\right] \quad (2)$$

$$\frac{\partial \rho \omega}{\partial t}+\frac{\partial u_i \rho \omega}{\partial x_i}=\rho\left[C_{\omega 1}\frac{\omega}{k}P_k+\left(\frac{C_{\omega R}}{f_W}-1\right)\frac{\omega}{k}(R_{BP}+R_{NAT})-C_{\omega 2}f_w^{\frac{4}{3}}\omega^2-C_{\omega 1}f_W\alpha_T f_w^2\frac{\sqrt{k}}{d^3}\right]+\frac{\partial}{\partial x_i}\left[\left(\mu+\frac{\rho\alpha_T}{\sigma_\omega}\right)\frac{\partial \omega}{\partial x_i}\right] \quad (3)$$

The parameter P_k and P_{kL} are both production terms of k and k_L:

$$P_k=\nu_{T,s}S^2 \quad (4)$$

$$P_{k_L}=\nu_{T,l}S^2 \quad (5)$$

The parameter $\nu_{T,s}$ and $\nu_{T,l}$ are the eddy viscosities of small scale and large scale, respectively. The sum of these values ($\nu_t = \nu_{T,s} + \nu_{T,l}$) is used for the eddy viscosity of the momentum equation. The parameter R_{BP} and R_{NAT} are the contributions of the bypass transition and the natural transition, respectively. The contribution of the bypass transition increases as the turbulent intensity in the external flow increases.

For the definitions of other variables and constants, please refer the references.

2.2 Modelling of Cavitating Flows

In this paper, relative motions between vapour and liquid are neglected since the flows are assumed to be uniform. In addition, a barotropic relation is used and the governing equations of mass and momentum are formally the same as those of the single phase flows.

Mixture density is described as follows:

$$\rho=\sum \alpha_N \rho_N \quad (6)$$

where, N denotes phase and α volume fraction. By using this mixture density, mass and momentum conservation equations are described as follows:

$$\frac{\partial \rho}{\partial t}+\frac{\partial \rho u_i}{\partial x_i}=0 \quad (7)$$

$$\frac{\partial \rho u_i}{\partial t}+\frac{\partial \rho u_i u_j}{\partial x_j}=-\frac{\partial P}{\partial x_i}+\frac{\partial \tau}{\partial x_j} \quad (8)$$

where, τ indicates shear stress.

Cavitating flows are applied as compressible flows. Thus the barotropic relation is employed to the equation of the state. Mixture density containing a non-condensable gas can be specified by mass fraction instead of volume fraction.

$$\frac{1}{\rho}=\frac{Y_v}{\rho_v}+\frac{Y_g}{\rho_g}+\frac{1-Y_v-Y_g}{\rho_l} \quad (9)$$

where, Y_v and Y_g denote mass fraction of vapour and a non-condensable gas, respectively. Mass fraction of a non-condensable gas is assumed to be constant analysis parameter. Density of the non-condensable gas is obtained by the following equation.

$$\rho_g=\frac{P}{RT} \quad (10)$$

where, R is a gas constant of the non-condensable gas and the flow field is assumed to be isothermal because temperature T is also a constant.

Mass fraction of vapour is calculated by the transport equation below.

$$\frac{\partial \rho Y_v}{\partial t}+\frac{\partial \rho u_i Y_v}{\partial x_i}=R_e-R_c \quad (11)$$

The right-hand side is source terms indicating evaporation and condensation which are modelled by the full-cavitation model (Singhal et al 2002).

$$R_e=C_e\frac{\sqrt{k}}{\sigma}\rho_l\rho_v\sqrt{\frac{2}{3}\frac{P_v-P}{\rho_l}}\left(1-Y_v-Y_g\right) \quad (12)$$

$$R_c=C_c\frac{\sqrt{k}}{\sigma}\rho_l\rho_l\sqrt{\frac{2}{3}\frac{P-P_v}{\rho_l}}Y_v \quad (13)$$

where, k denotes turbulent kinetic energy, ρ_l and ρ_v density of liquid and vapor, respectively, and σ surface tension coefficient. In the full cavitation model, the effect of turbulence is taken into account for the threshold of pressure, P_v, where evaporation occurs.

$$P_v=P_s+\frac{0.39\rho k}{2} \quad (14)$$

where, P_s indicates the saturation pressure. The model constants are $C_e = 0.02$ and $C_c = 0.01$.

3 ANALYSIS OF OPEN WATER TESTS

The open water tests conditions and the propeller model geometry were given by SMP'11 workshop. Table 1 and Figure 1 show the main characteristics and propeller shape of *PPTC* which is the propeller for the calculation. The analysis conditions are listed in Table 2.

Figure 2 shows the computational domain which comprises the inner rotational part containing the propeller, and the outer stationary part whose size is the same as the size of the towing tank. The inner rotational part and outer stationary part connect discontinuously. The inlet/outlet boundary is in the stationary part, and the constant velocity and zero pressure conditions are applied to it. In this analysis, the simulation is operated as the

steady-state analysis. The inner rotational part is not actually rotated. Instead, the rotation is converted to the force which is applied to the part.

For transitional flow simulations, LKE k-k_L-ω turbulence model is used. SIMPLEC method is used for coupling between pressure and mass conservation. Convection terms appeared in each equation is discretized by the second order upwind method.

The numerical mesh is an unstructured grid which comprises tetrahedral basic cells and prismatic cells for resolving the boundary layer around the surface. Figure 3 shows the mesh used in this analysis and Table 3 lists the number of nodes and elements. In this analysis, LKE k-k_L-ω turbulence model was used and $y^+ < 1$ is highly recommended to use this model. Therefore, the first layer meshes around the surface were generated to satisfy this recommendation.

The computed results of open water tests are shown in Figure 4. The thrust coefficient K_T and the torque coefficient K_Q decrease when the advance coefficient J increases. On the other hand, the open water efficiency η_0 increases when J increases. However, the increase of J slows down when its value exceeds 1. Figure 5 shows limiting streamlines of two advance coefficients J = 0.6 and 1.4. The effect of the transition is shown in these figures.

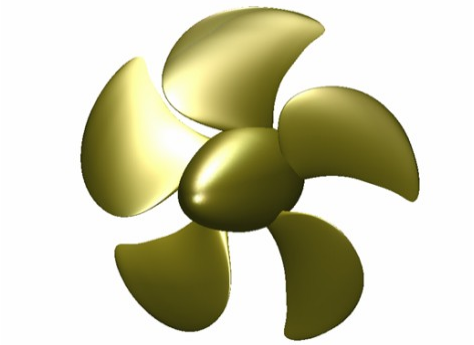

Figure 1 PPTC propeller

Table 1 Principal particular of PPTC propeller

Number of Blades	5
Diameter [m]	0.25
Pitch Ratio at 0.7R	1.635
Skew [deg]	18.8

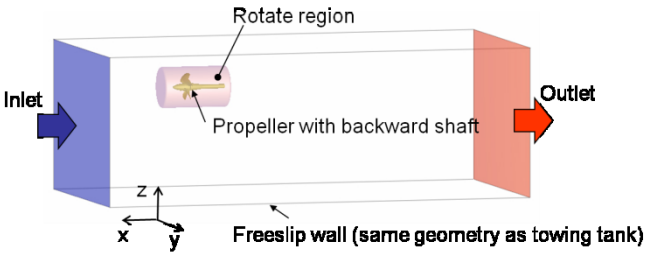

Figure 2 Computational domains of open water tests

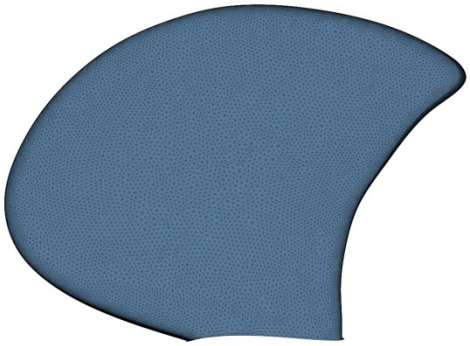

Figure 3 Computation mesh on propeller surface

Table 2 Condition of mesh for open water tests

Total Node Number	10000000
Total Element Number	28000000
y^+	< 1
Prism Layers	20

Table 3 Condition of open water tests

Rate of revolutions [1/s]	n	12
Water Tempreture [degC]	T	17.5
Water Density [kg/m^3]	ρ	998.68
Kinematic viscosity of water [m^2/s]	ν	1.07E-06
Advance corfficients	J	0.6 - 1.4
Inlet Velocity [m/s]	V_A	2.25 - 5.25

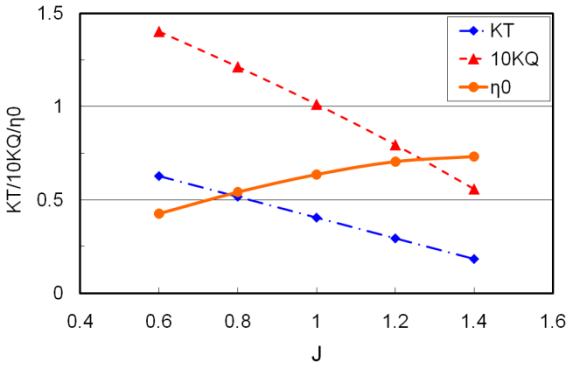

Figure 4 Computed characteristics of PPTC propeller

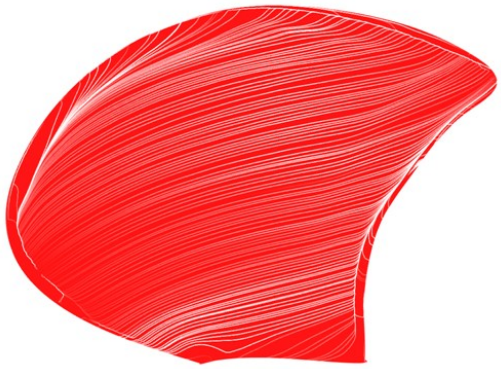

(a) J = 0.6

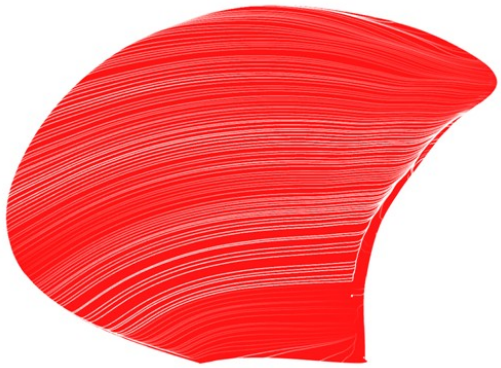

(b) J = 1.4

Figure 6 Limiting streamlines of PTCC propeller

4 ANALYSIS OF TIP VORTEX

The velocity field tests conditions of the cavitation tunnel shown Table 4 were also given by the workshop. Figure 6 shows the computational domain and the outer stationary part size was adjusted to be the same as that of the cavitation tunnel.

Realizable *k*-ε model is used for the turbulence model and SIMPLEC method is used for coupling between pressure and mass conservation.

Figure 7 and Table 5 show the computational mesh and the number of nodes and elements. In this analysis, the mesh of the first layer were generated with y^+ = 30, because high-Reynolds-type turbulence model was used. In addition, adequately fine meshes behind the tip of one blade of the propeller were generated to achieve high resolution of tip vortex.

The velocity fields to a distance of x/D = 0.1, r/R = 1.0 and x/D = 0.2, r/R = 0.97 are shown Figure 8. In Figure 8(a), the peak of the velocity was observed near -30 degrees. In addition, the peak of the velocity was also observed near 20 degrees in figure 8(b). These results show that tip vortex was correctly computed to a distance of x/D = 0.2 in this analysis.

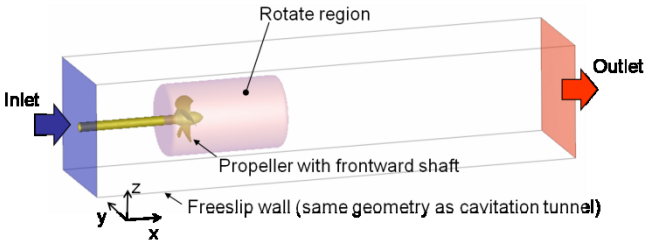

Figure 5 Computational domain of tip vortex and cavitating analyses

Table 4 Conditions of velocity field test

Rate of revolutions [1/s]	n	23
Water Tempreture [degC]	T	24.7
Water Density [kg/m^3]	ρ	997.1
Kinematic viscosity of water [m^2/s]	ν	9.03E-07
Advance corfficients	J	1.253
Inlet Velocity [m/s]	V_A	7.204
Thrust coefficient	K_T	0.25
Torque coefficient	$10K_Q$	0.725

Table 5 Condition of mesh for tip vortex and cavitating analyses

Total Node Number	6000000
Total Element Number	23000000
y^+	30
Prism Layers	5

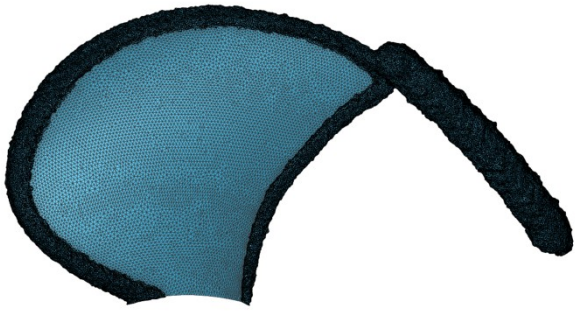

Figure 7 Computation mesh on propeller surface and fine mesh region

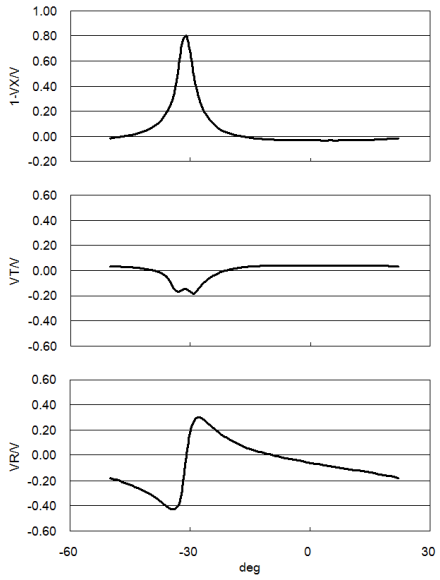

(a) x/D = 0.1, r/R = 1.0

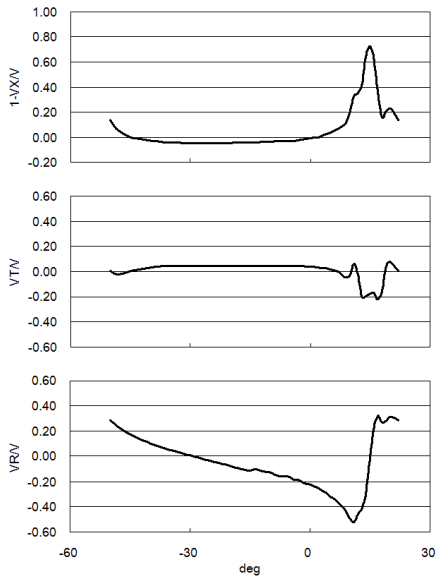

(b) x/D = 0.2, r/R = 0.97

Figure 8 Velocity field behind propeller

5 ANALYSIS OF CAVITATING FLOWS

The results of cavitating flow tests of the computational domain were the same as those of the analyses of tip vortex. The computational mesh cavitating flow tests were also the same as that of tip vortex analyses.

In this analysis, the full-cavitation model was used for cavitating flow analyses, while SIMPLER method was used for coupling between pressure and mass conservation. In SC/Tetra, cavitating flows were calculated as compressible flows. RNG k-ε turbulence model was used. The analysis parameters required in the full-cavitation model were mass fraction of the non-condensable gas (air) $Y_a = 10^{-6}$, and surface tension σ = 0.07275.

The analysis conditions of each test case were listed in Table 6.

Figure 9 shows cavity patterns on the blade of each test case. In Case 1, cavitation was observed on the leading edge of the suction side and on the tip vortex region. In Case 2, cavitation was generated on the tip vortex region and at the middle of the suction surface. In Case 3, cavitation was generated only on the leading edge of the pressure side.

The thrust coefficients K_T of the cavitating propeller in each test case were shown in Table 7. Figure 10 shows pressure distribution on the propeller blade surface in the non-cavitating and cavitating states.

Table 6 Test conditions of cavitating flows

Test Case		Case1	Case2	Case3
Rate of revolutions [1/s]	n	24.897	24.986	25.014
Water Tempreture [degC]	T	23.2	23.2	23.2
Water Density [kg/m^3]	ρ	997.44	997.44	997.37
Vapour Pressure [Pa]	p_v	2818	2818	2869
Kinematic viscosity of water [m^2/s]	ν	9.34E-07	9.34E-07	9.73E-07
Advance corfficients	J	1.019	1.269	1.408
Inlet Velocity [m/s]	V_A	6.365	7.927	8.805
Thrust coefficient (non-cavitating)	K_T	0.387	0.245	0.167
Cavitation number	σ_n	2.024	1.424	2.000

Table 7 Calculation results of cavitating propeller thrust coefficient

Test Case		Case 1	Case 2	Case 3
Thrust coefficient	K_T	0.375	0.199	0.138

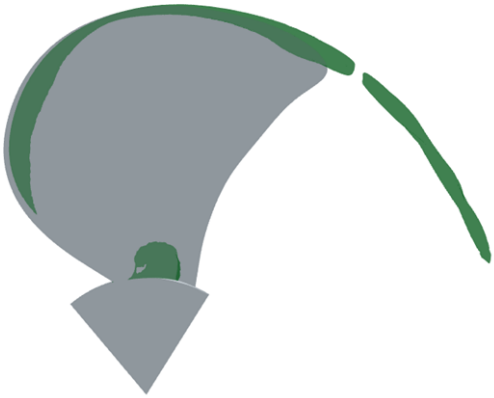

(a) Case1, Suction side

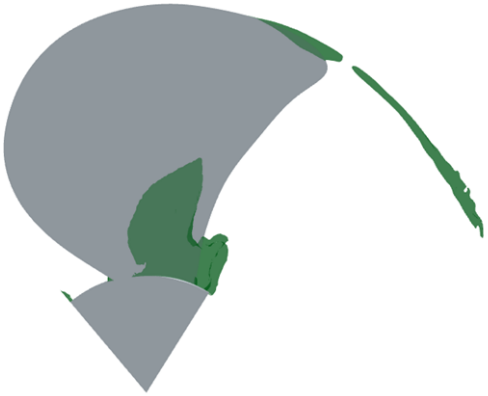

(b) Case2, Suction side

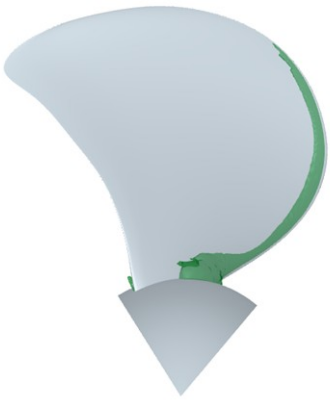

(c) Case3, Pressure side

Figure 9 Calculated cavity pattern (volume fraction of 20% of vapour)

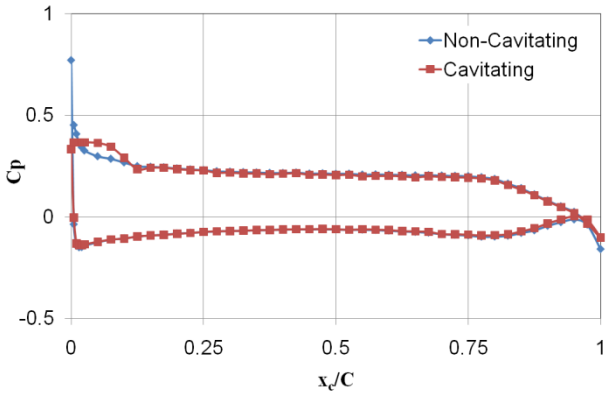

(a) Case1

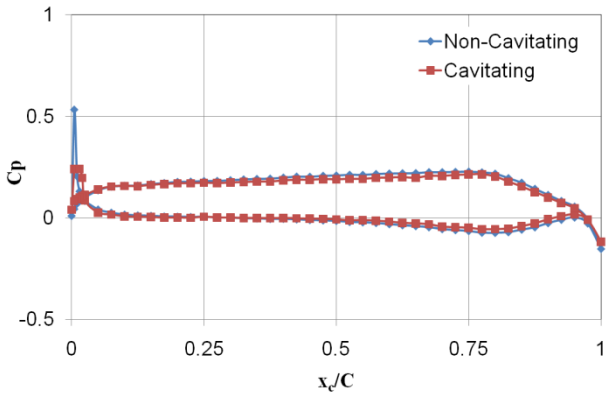

(b) Case2

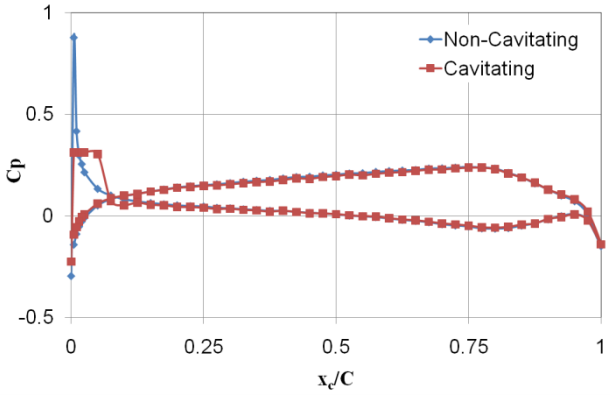

(c) Case3

Figure 10 Pressure distributions on the propeller surface (r/R = 0.7)

6 CONCLUSION

SC/Tetra, RANS-based CFD code, showed the significant effectiveness in the numerical simulations of both non-cavitating and cavitating analyses of the marine propellers based on the results of the problems provided by SMP'11 workshop.

(1) The transitional flows in the open water tests of marine propeller were obtained effectively by using the RANS based LKE k-k_L-ω model.

(2) The cavitating flows of the propeller were obtained usefully by using the RANS model and the full-cavitation model together.

(3) Generating fine mesh behind the tip of blades enabled the high-resolution in tip vortex calculations. In addition, the computations of the tip vortex cavitation were also obtained

NOMENCLATURE

J	Advance coefficient $(= V/nD)$
K_T	Thrust coefficient $(= T/\rho n^2 D^4)$
K_Q	Torque coefficient $(= Q/\rho n^2 D^5)$
η_0	Open water efficiency $(= J \cdot K_T/2\pi \cdot K_Q)$
σ_n	Cavitation number $(= (p - p_v)/0.5 \cdot \rho(nD)^2)$
C_p	Pressure coefficient $(= (p - p_0)/0.5 \cdot \rho\{V^2 + (2\pi nr)^2\})$

REFERENCES

Singhal, A. K., Athavale, M. M., Li, H., Jiang, Y. (2002). 'Mathematical basis and validation of the full cavitation model', Journal of Fluids Engineering **124**, pp.617-624.

Walters, D.K., Leylek, J.H. (2004).

'A New Model for Boundary Layer Transition Using a Single-Point RANS Approach', ASME Journal of Turbomachinery, 126, pp.193-202,

Walters, D.K., Cokljat, D.(2008).

'A Three-Equation Eddy-Viscosity Model for Reynolds-Averaged Navier-Stokes Simulations of Transitional Flow', ASME J. of Fluids Eng., 130, 121401